

*20p.*



N 6 8 1 0 0 0 4

*code - 1*

# TECHNICAL NOTE

D-1848

## TESSERAL HARMONICS OF THE GRAVITATIONAL FIELD AND GEODETIC DATUM SHIFTS DERIVED FROM CAMERA OBSERVATIONS OF SATELLITES

William M. Kaula  
Goddard Space Flight Center  
Greenbelt, Maryland

NATIONAL AERONAUTICS AND SPACE ADMINISTRATION  
WASHINGTON

June 1963

Note!

**CALCULATED**

# TESSERAL HARMONICS OF THE GRAVITATIONAL FIELD AND GEODETIC DATUM SHIFTS DERIVED FROM CAMERA OBSERVATIONS OF SATELLITES

by  
William M. Kaula  
*Goddard Space Flight Center*

## SUMMARY

16994

Baker-Nunn Camera observations of satellites 1959  $\alpha 1$  over 315 days, 1959  $\eta$  over 105 days, and 1960  $\iota 2$  over 294 days were analyzed for 35 spherical harmonic coefficients of the earth's gravitational field and for position shifts of six geodetic datums. Of the three satellites, only 1960  $\iota 2$  appeared to have a sufficiently good observation distribution and small enough drag effects to yield significant results.

The datum shifts obtained have standard deviations averaging  $\pm 25$  m in each coordinate. The gravitational harmonic coefficients obtained appear to be appreciably different from zero for indices (n, m) at (2,2), (3,1), (4,1) and (4,3). In particular, geophysically significant magnitudes were obtained for  $\bar{J}_{22} : 2.51 \times 10^{-6}$  and  $\bar{J}_{31} : 1.79 \times 10^{-6}$  (normalized).



## CONTENTS

Summary . . . . .	i
INTRODUCTION. . . . .	1
OBSERVATIONS. . . . .	1
GEOMETRY . . . . .	2
DYNAMICS . . . . .	3
DATA ANALYSIS. . . . .	8
RESULTS AND CONCLUSIONS. . . . .	13
ACKNOWLEDGMENTS . . . . .	14
References . . . . .	16



# TESSERAL HARMONICS OF THE GRAVITATIONAL FIELD AND GEODETIC DATUM SHIFTS DERIVED FROM CAMERA OBSERVATIONS OF SATELLITES\*

by

William M. Kaula

*Goddard Space Flight Center*

## INTRODUCTION

The Baker-Nunn Camera observations described by Veis (References 1 and 2) and Haramundanis (Reference 3) will be analyzed by the methods described in References 4-7. Solutions were made for all geodetic and gravitational parameters estimated to have effects of more than  $\pm 20$  meters on satellite orbits. The intent of the analysis was to apply all devices short of allowing for covariance of observations at different times. This intent resulted in programs complicated enough that most of the time spent was consumed by purely computational difficulties. An IBM 7090 computer was used.

## OBSERVATIONS

The Baker-Nunn Camera system, its accuracy, and operation by the Smithsonian Institution Astrophysical Observatory are described by Henize (Reference 8), Lassovszky (Reference 9), Weston (Reference 10), Veis and Whipple (Reference 11). That the random error of the plate measurements is of the order of  $\pm 2''$  has been confirmed in this analysis by accuracy with which a line can be fitted to plotted residuals with respect to an orbit of observations close together in the same pass. Since the significant timing error is virtually constant throughout a pass, no such test of timing errors is possible because of the dominant effect of drag error in the orbit.

The Baker-Nunn Camera observations as published by Veis (References 1 and 2) and Haramundanis (Reference 3) are referred to the 1950 mean positions of the stellar catalogue. For this analysis, the epoch of the right ascension and declination was updated to the epoch of the orbital arc fitted to the observations, taking into account precession plus nutational terms of more than  $0''.25$  amplitude — i.e., the 18.6 year and semi-annual terms. A.1 times are given for the observations and are treated as equivalent to ephemeris time. A small correction was applied in calculating Greenwich Sidereal Times (GST) to allow for the precession and nutation between the epoch of the orbital arc and the instant of observation.

---

\*This paper was published in substantially the same form in *J. Geophys. Res.* 68(2):473-484, January 15, 1963.

The above mentioned  $\pm 2''$  accuracy of fitting of a line to residuals is appreciably smaller than the residuals themselves, which indicates that extra observations within a pass did not add extra weight to the orbit analysis. Hence, to conserve computer time and to avoid overweighting certain passes, observations were omitted which were neither terminal observations of a pass nor observations interior to a pass at intervals of 2 minutes or more.

The final rejection criterion applied was to omit observations on days of appreciable atmospheric disturbance, as measured by the geomagnetic index  $A_p$ . For the 1960  $\alpha 2$  (Echo I rocket body) analysis, observations were omitted on days for which  $A_p$  exceeded 50; for 1959  $\alpha 1$  (Vanguard II and 1959  $\eta$  (Vanguard III), when  $A_p$  exceeded 70. In some cases additional observations on adjacent days were omitted to prevent an orbital arc from bridging across days of high  $A_p$  index.

The principal defect in the observations is, of course, their poor distribution due to the dependence on reflected sunlight; to the limited number of tracking stations – twelve; and, in the case of 1959  $\alpha 1$  and 1959  $\eta$ , to the closeness of the satellite perigees.

## GEOMETRY

The observation equation used was in terms of the meridian and prime vertical components of the plate measurement, assuming that the satellite was on the camera axis (References 4 and 12), and consists of the first two rows of the matrix equation:

$$\begin{Bmatrix} d\delta \\ d\alpha \cos \delta \\ \frac{dr}{r} \end{Bmatrix} = \left\{ \frac{d\mathbf{b}}{r} \right\}_{obs} = - \left\{ \frac{\mathbf{b}}{r} \right\}_{obs} + \frac{\mathbf{R}_{bx} \{ \mathbf{R}_{xq} \mathbf{q} + \mathbf{C}_{xe} d\mathbf{e} + \mathbf{C}_{xm} n dt - \mathbf{R}_3 (-\theta) d\mathbf{u}_0 \}}{r}, \quad (1)$$

where  $\delta$  is the declination,  $\alpha$  the right ascension,  $r$  the camera-satellite range. In Equation 1, the first two rows of  $(\mathbf{b}/r)_{obs}$  are zero, if the observed  $\delta$ ,  $\alpha$  are used in  $\mathbf{R}_{bx}$ , the rotation matrix from the inertial coordinate system to a rectangular system with the 3-axis coincided with the camera-satellite line, and the 1-axis in the meridian;  $\mathbf{q}$  is the satellite position in orbit-referred coordinates, with the 1-axis toward osculating perigee and the 3-axis normal to the osculating orbit;  $\mathbf{R}_{xq}$  is the rotation from orbit-referred to inertial coordinates;  $\mathbf{C}_{xe}$  is a  $3 \times 6$  matrix of partial derivatives of the inertial rectangular coordinates with respect to the osculating Keplerian elements, corrections to which are symbolized by  $d\mathbf{e}$ ;  $\mathbf{C}_{xm}$  is the row of  $\mathbf{C}_{xe}$  corresponding to the mean anomaly;  $n$  is the mean motion;  $dt$  is a correction to the time of observation;  $\mathbf{R}(-\theta)$  is the geodetic to inertial rotation matrix, with the Greenwich Sidereal Time  $\theta$  as argument; and  $d\mathbf{u}_0$  is a vector of corrections to station position. (Derivations of all these variables are given in Equations 46, 47, 52-60 of Reference 4, or Equations 3.1-3.8, 3.11-3.15 of Reference 12.)

The partial derivatives in Equation 1,

$$\mathbf{C}_t = \begin{Bmatrix} \frac{\partial \delta}{\partial t} \\ \frac{\partial (\alpha \cos \delta)}{\partial t} \end{Bmatrix} = \begin{Bmatrix} 1, & 0, & 0 \\ 0, & 1, & 0 \end{Bmatrix} \frac{\mathbf{R}_{bx} \mathbf{C}_{xm}}{r} n, \quad (2)$$

were not actually used to determine timing corrections; but were used for three other purposes: (1) A correction  $rC_t/c$  was applied for the time of travel of the signal ( $c$  is the velocity of light); (2) a lower weight was given to the along-track component than to the across-track component of the observation, by giving each observation a  $2 \times 2$  covariance matrix,

$$V_{obs} = \begin{Bmatrix} \sigma_d^2 & 0 \\ 0 & \sigma_t^2 \end{Bmatrix} + C_t \sigma_t^2 C_t^T, \quad (3)$$

where  $\sigma_d^2$  is the variance of the direction measurement,  $\sigma_t^2$  is the variance of the timing, and the superscript T denotes transpose; and (3) the residuals in along-track and cross-track components were computed by applying to  $(\delta, a \cos \delta)$  residuals the rotation:

$$R_{ti} = \begin{Bmatrix} \frac{C_1}{\sqrt{C_1^2 + C_2^2}}, & \frac{C_2}{\sqrt{C_1^2 + C_2^2}} \\ -C_2 & C_1 \end{Bmatrix}, \quad (4)$$

where  $C_1, C_2$  are the two elements of  $C_t$ .

Consistent with the assumption, stated in the introduction, of seeking all effects expected to be larger than  $\pm 20$  m, all stations were assumed to have position error, but those stations connected to the same geodetic system were assumed to shift together. Hence the twelve cameras were referred to six datums: four to the Americas (Am) system; four to the Europe-Africa-Siberia-India (EASI) system; and one each to the Australian (Au), Japan-Korea-Manchuria (JKM), Argentine (Ar), and Hawaiian (H) systems. For the Am, EASI, JKM systems, the starting station positions were those obtained in the solution for a world geodetic system of Kaula (Reference 13). For the Au, Ar, and H systems the positions calculated by Veis (Reference 14) were taken and shifted by placing tangent to the datum origin an ellipsoid of flattening  $1/298.3$  and an equatorial radius of  $6378165 + N_0$  m, where  $N_0$  is the geoid height in the vicinity of the datum origin as given by Kaula (Reference 13). The initial station positions are given in Table 1, in length units of 6.378165 m referred to the U coordinate system, with axes toward  $0^\circ, 0^\circ$ ;  $0^\circ, 90^\circ\text{E}$ ; and  $90^\circ\text{N}$  respectively.

## DYNAMICS

Variables in the observation equation (Equation 1) dependent on the dynamics of the satellite orbit are:

$$R_{xq} = R_3(-\Omega) R_1(-i) R_3(-\omega) \quad (5)$$

Table 1  
Tracking Station Data in Length Units of 6.378165 m

Station	Latitude and Longitude (degrees)	Datum	Starting Coordinates	Preassigned $\sigma$	Solution	
					Preliminary	Final
Organ Pass	32.4	Americas	-240778.9	$\pm 3.0$	-14.8	- 2.8 $\pm$ 0.9
	253.4		-810109.7	$\pm 3.9$	- 5.6	- 3.8 $\pm$ 1.8
			+533234.2	$\pm 3.1$	+ 3.3	- 0.2 $\pm$ 1.0
Arequipa	-16.5		+304591.7			
	288.5		-909989.8			
			-281725.5			
Curacao	12.1		+353051.9			
	291.2		-912004.8			
			+208079.7			
Jupiter	27.0		+153068.1			
	279.8		-878214.3			
			+451581.1			
Olifants- Fontein	-26.0	Europe- Africa- Siberia- India	+792726.2	$\pm 3.4$	+16.3	+ 5.4 $\pm$ 1.3
	28.3		+425915.7	$\pm 2.9$	-17.8	- 8.0 $\pm$ 1.4
			-435196.6	$\pm 2.9$	+ 0.1	+ 2.6 $\pm$ 2.5
San Fernando	36.5		+800481.9			
	353.8		- 87033.6			
			+591042.3			
Naini Tal	29.4		+159627.8			
	79.5		+857813.2			
			+487527.7			
Shiraz	29.6		+529444.8			
	52.5		+690490.0			
			+491723.2			
Woomera	-31.1	Australia	-624562.7	$\pm 11.3$	+ 6.4	-15.0 $\pm$ 4.0
	136.8		+586884.9	$\pm 14.5$	+14.5	+ 4.4 $\pm$ 8.3
			-513573.3	$\pm 13.2$	+ 2.8	+ 8.7 $\pm$ 6.5
Tokyo	35.7	Japan- Korea- Manchuria	-618774.5	$\pm 5.2$	0.0	- 8.5 $\pm$ 2.7
	139.5		+527787.3	$\pm 6.9$	+15.2	+ 6.8 $\pm$ 3.4
			+579917.5	$\pm 5.2$	+ 1.9	+ .9 $\pm$ 2.4
Villa Dolores	-31.9	Argentina	+357509.6	$\pm 28.4$	+27.1	+36.9 $\pm$ 3.9
	294.9		-770550.4	$\pm 22.8$	- 2.2	+ 3.4 $\pm$ 5.0
			-526083.5	$\pm 26.2$	+ 1.2	+ 3.3 $\pm$ 6.6
Maui	20.7	Hawaii	-857008.8	$\pm 21.7$	+ 1.8	+ 1.5 $\pm$ 6.1
	203.7		-376954.1	$\pm 35.8$	+28.5	+14.1 $\pm$ 7.9
			+351587.3	$\pm 37.1$	-53.3	-50.1 $\pm$ 4.7

and

$$\mathbf{q} = \begin{Bmatrix} a (\cos E - e) \\ a \sqrt{1-e^2} \sin E \\ 0 \end{Bmatrix} \quad (6)$$

where  $E, a, e, i, \omega, \Omega$  are the osculating eccentric anomaly, semi-major axis, eccentricity, inclination, argument of perigee, and longitude of the ascending node, respectively; and

$$d\mathbf{e} = \mathbf{J} d\mathbf{e}_0' + \mathbf{C}_{eg} d\mathbf{p}_g + \mathbf{C}_{et} d\mathbf{p}_t + \mathbf{C}_{ed} d\mathbf{p}_d + \mathbf{C}_{ep} d\mathbf{p}_p \quad (7)$$

where  $\mathbf{e}_0'$  denotes the elements of an intermediate orbit at epoch;  $\mathbf{p}_g$ , parameters expressing variations in the earth's gravitational field (such as spherical harmonic coefficients);  $\mathbf{p}_t$ , arbitrary polynomials of the Keplerian elements;  $\mathbf{p}_d$ , parameters of an atmospheric model and the interaction therewith of the satellite; and  $\mathbf{p}_p$ , parameters expressing radiation pressure effects.

The procedure used to compute the osculating elements  $M, a, e, i, \omega, \Omega$  and the partial derivatives matrices  $\mathbf{J}, \mathbf{C}_{eg}, \mathbf{C}_{et}, \mathbf{C}_{ed}, \mathbf{C}_{ep}$  was as follows.

Preliminary orbits were determined by iterated differential correction fit to the observations based on the parameters: (1) the constants of integration of the orbital theory of Brouwer (Reference 15); (2) the gravitational field parameters  $\kappa M$ , and zonal harmonics  $J_2, J_3, J_4$ ; and (3) arbitrary polynomials in time of the Keplerian elements. The principal purpose of this preliminary orbit determination was to obtain osculating elements at the instant of each observation close enough to the true values that the corrections could be considered linear.

The intermediate orbit elements defining the preliminary orbit were used to generate Fourier series expressing the effects of the several perturbations and the partial derivatives of the osculating elements with respect to the parameters of the perturbations.

For  $\mathbf{C}_{eg}$ , the effect of spherical harmonics of the earth's gravitational field, the disturbing function developed in Kaula (Reference 4) was used:

$$R_{nm} = \frac{a_e^n \mu}{a^{n+1}} \sqrt{\frac{(n-m)! (2n+1) \kappa_m}{(n+m)!}} \sum_{p=0}^n F_{nmp}(i) \sum_{q=-\infty}^{\infty} G_{npq}(e) \cdot \left[ \begin{aligned} & \left\{ \begin{array}{l} \bar{C}_{nm} \\ -\bar{S}_{nm} \end{array} \right\}_{(n-m) \text{ even}}^{(n-m) \text{ even}} \cos \{ (n-2p)\omega + (n-2p+q)M + m(\Omega-\theta) \} \\ & + \left\{ \begin{array}{l} \bar{S}_{nm} \\ \bar{C}_{nm} \end{array} \right\}_{(n-m) \text{ odd}}^{(n-m) \text{ even}} \left\{ \begin{array}{l} \bar{S}_{nm} \\ \bar{C}_{nm} \end{array} \right\}_{(n-m) \text{ odd}}^{(n-m) \text{ odd}} \sin \{ (n-2p)\omega + (n-2p+q)M + m(\Omega-\theta) \} \end{aligned} \right] \quad (8)$$

where  $\kappa_0 = 1$ ;  $\kappa_m = 2$ ,  $m \neq 0$ .

This disturbing function was used in the Lagrangian equations of motion (Reference 16, p. 289) and integrated under the assumption that  $a, e, i$  remained constant and  $M, \omega, \Omega$  changed secularly. The

program automatically determined for each spherical harmonic all terms above a specified minimum, in absolute magnitude, and stored the results as subscripted numerical arrays to be multiplied by the sines and cosines evaluated at the instant of each observation. An example of one of the 210 such partial derivatives formed for satellite 1960 2 is

$$\begin{aligned} \frac{\partial e}{\partial \bar{C}_{31}} = & 1.850 \cos (\omega + \Omega - \theta) - 0.001 \cos (\omega + M + \Omega - \theta) + 5.058 \cos (-\omega + \Omega - \theta) \\ & + 0.002 \cos (-\omega - M + \Omega - \theta) - 0.609 \cos (-\omega - 2M + \Omega - \theta) . \end{aligned} \quad (9)$$

By using a rejection criterion of  $0.1 n^{1.2}$  and applying it to partial derivatives of the elements  $M + \omega + \Omega \cos i$ ,  $e^2 (\omega + \Omega \cos i)$ ,  $\Omega \sin i$ ,  $e$ ,  $i$ , and  $a$  between 1 and 6 significant periodicities were found for each term.

The harmonics listed in Table 2 were selected on the basis that they had a rms anticipated effect on the satellite orbit of  $\pm 20$  m or more, using the degree variances given in Reference 17.

As expected, the partial derivatives indicated poor separation of even degree harmonics of the same order  $m$ . However, the effect of the different frequency odd - especially 3rd - degree harmonics was unexpectedly distinct. The even degree harmonics caused principally along-track perturbations of frequency  $m (\dot{\Omega} - \dot{\theta})$ , while the odd degree harmonics perturbed mainly the eccentricity (or perigee height) for a nearly circular orbit.

For tesseral harmonic coefficients, initial values of zero were assumed; for zonal harmonic coefficients, the values of Kozai (Reference 18) were used. For the gravitational effects of the sun and moon, the similar disturbing function in Reference 19 was used. All secular terms were retained, plus periodic terms of more than  $2 \times 10^{-5}$  amplitude, of which 2 to 9 were found for each orbit. For the radiation pressure effect of the sun, the disturbing function in Reference 19 was used. Because of the irregular effect of the earth's shadow, the perturbations were not integrated analytically, and a numerical harmonic analysis was applied instead. A harmonic analysis interval of 15 days (or minimum period of 30 days) was found sufficient to reflect all variations of more than  $2 \times 10^{-5}$  amplitude. Partial derivatives were formed only for one parameter: the mean (reflectivity X cross-sectional area).

For drag, the effect of an empirical atmospheric model was applied with density in the form (Reference 20):

$$\rho = \rho_0 \left( \frac{S}{100} \right)^m \exp \left\{ \frac{h - h_0}{H} + c e^{-dh} \right\} \left\{ 1 + b (e^{ah} - k) \cos^n \frac{\psi}{2} \right\} . \quad (10)$$

In Equation 10,  $S$  is the solar flux of 10.7 (or 20) cm wave length,  $h$  is the height above the earth's surface, and  $\psi$  is the angle from the center of the diurnal bulge and is determined by

$$\cos \psi = \frac{\{1, 0, 0\} R_3 (\lambda^*) R_1 (\epsilon) R_3 (\chi) R_{\text{axi}} q}{r} , \quad (11)$$

Table 2

Gravitational Coefficient Data (All numbers multiplied by a scaling factor of  $10^{-6}$ )

Gravitational Coefficient*	Starting Value	Preassigned $\sigma$	Solution		Gravitational Coefficient*	Starting Value	Preassigned $\sigma$	Solution		Preliminary	Final
			Preliminary	Final				Preliminary	Final		
$\Delta \bar{C}_{00}^{\dagger}$	.00	$\pm 10.00$	4.52	$1.23 \pm 3.29$	$\bar{C}_{43}$	.00	$\pm .63$	1.23	$.50 \pm .21$		
$\Delta \bar{C}_{20}^{\dagger}$	-.054	$\pm .07$	.01	$-.06 \pm .01$	$\bar{S}_{43}$	.00	$\pm .63$	.10	$.16 \pm .19$		
$\bar{C}_{21}$	.00	$\pm 2.00$	-.04	Fixed	$\bar{C}_{44}$	.00	$\pm .63$	-.48	$-.24 \pm .27$		
$\bar{S}_{21}$	.00	$\pm 2.00$	-.07	Fixed	$\bar{S}_{44}$	.00	$\pm .63$	1.12	$.55 \pm .29$		
$\bar{C}_{22}$	.00	$\pm 2.00$	2.96	$1.84 \pm .19$	$\bar{C}_{50}$	.019	$\pm .02$	-.30	$.03 \pm .01$		
$\bar{S}_{22}$	.00	$\pm 2.00$	-1.71	$-1.71 \pm .28$	$\bar{C}_{51}$	.00	$\pm .39$	.35	$.08 \pm .14$		
$\bar{C}_{30}$	.970	$\pm .02$	1.07	$.98 \pm .01$	$\bar{S}_{51}$	.00	$\pm .39$	.70	$.26 \pm .15$		
$\bar{C}_{31}$	.00	$\pm 1.26$	1.89	$1.77 \pm .21$	$\bar{C}_{60}$	-.110	$\pm .10$	.00	$-.10 \pm .02$		
$\bar{S}_{31}$	.00	$\pm 1.26$	.28	$-.11 \pm .20$	$\bar{C}_{61}$	.00	$\pm .28$	.06	$.02 \pm .08$		
$\bar{C}_{32}$	.00	$\pm 1.26$	-.37	$.34 \pm .26$	$\bar{S}_{61}$	.00	$\pm .28$	-.05	$-.18 \pm .07$		
$\bar{S}_{32}$	.00	$\pm 1.26$	.30	$.08 \pm .35$	$\bar{C}_{62}$	.00	$\pm .28$	.21	$.00 \pm .06$		
$\bar{C}_{33}$	.00	$\pm 1.26$	-.32	$-.31 \pm .46$	$\bar{S}_{62}$	.00	$\pm .28$	.07	$.06 \pm .07$		
$\bar{S}_{33}$	.00	$\pm 1.26$	.61	$.74 \pm .46$	$\bar{C}_{63}$	.00	$\pm .28$	1.11	$.13 \pm .08$		
$\bar{C}_{40}$	.613	$\pm .12$	.79	$.55 \pm .10$	$\bar{S}_{63}$	.00	$\pm .28$	.31	$.21 \pm .16$		
$\bar{C}_{41}$	.00	$\pm .63$	-.10	$-.21 \pm .16$	$\bar{C}_{64}$	.00	$\pm .28$	.00	$.13 \pm .11$		
$\bar{S}_{41}$	.00	$\pm .63$	.60	$.46 \pm .15$	$\bar{S}_{64}$	.00	$\pm .28$	-.28	$-.24 \pm .10$		
$\bar{C}_{42}$	.00	$\pm .63$	.66	$-.03 \pm .19$	$\bar{C}_{70}$	.121	$\pm .02$	-.13	$.10 \pm .01$		
$\bar{S}_{42}$	.00	$\pm .63$	.25	$.32 \pm .19$							

\*  $\bar{C}_{nm}, \bar{S}_{nm}$  are coefficients of the spherical harmonic terms  $kW/r(a_e/r)^n H_{nm}$  such that  $\int H_{nm}^2 d\sigma = 4\pi$  for integration over the sphere (Reference 17, Equations 16-18).

$\dagger \Delta \bar{C}_{00}, \Delta \bar{C}_{20}$  are corrections to  $0.3986032 \times 10^{21}$  ( $1.0 - 0.00108236 P_2$ ) cgs.

where  $\lambda^*$  is the sun's longitude,  $\epsilon$  the inclination of the ecliptic, and  $\chi$  is the lag of the atmospheric bulge behind the sun.

The atmosphere was assumed to rotate with the solid earth, and to have the corresponding oblateness for a fluid. The customary assumption of the drag force being proportionate to the square of the velocity was made. The force components (radial, transverse, and normal to the satellite and its orbital plane) were used in the Gaussian equations of motion (Reference 16, p. 301) and in numerical Fourier series developed for the effects on the Keplerian elements. In generating these series, second-order effects on the angular elements dependent on the secular motions due to the oblateness were included. With an analysis interval of 3 days, variations as small as  $3 \times 10^{-6}$  amplitude were obtained in M.

For satellites 1959  $\alpha 1$  and 1959  $\eta$  the values of the parameters in Equation 9 as determined by Jacchia (Reference 20) were used. For satellite 1960  $\alpha 2$ ,  $c$ ,  $a$ , and  $k$  were set equal to zero, and  $\rho_0$ ,  $m$ ,  $H$ ,  $b$ ,  $n$ , and  $\chi$  were determined so as to fit the atmospheric models of Harris and Priester (Reference 21). For 1959  $\alpha 1$  and 1959  $\eta$ , the Jacchia model absorbed most of the long period drag variations, but did not fit variations characterized by periods of less than 10 days. For 1960  $\alpha 2$ , the Harris and Priester model did not reduce residuals significantly, and had a negligible effect on the values determined for the geodetic parameters; hence the model was omitted.

In computing the effects of arbitrary polynomials or the partial derivatives with respect thereto, the second-order effects of the acceleration based on the assumption of constant perigee height (Equations 5-14 of Reference 22; Equation 2.100 of Reference 12) were applied.

In the partial derivatives  $J$  with respect to the intermediate orbital elements at epoch (Equation 7), the effects of secular motions due to oblateness were included (Reference 4, Equation 49). To assure that the  $\pm 20m$  specification was met, the extension of Brouwer's theory to periodic terms of order  $J_2^2$  by Kozai (Reference 23) was examined but was found not to be needed.

In the final orbit analysis, the various perturbations were added to the osculating elements as determined from the preliminary orbit at each observation. To keep these preliminary positions close to the actual positions, the longer period drag and radiation pressure effects were subtracted from the arbitrary polynomials of the preliminary orbit. Provision was also made to eliminate any specified polynomials in the final orbit determination.

Orbital elements for the initial epoch, and other specifications, of each satellite are given in Table 3.

## DATA ANALYSIS

As discussed in References 5, 6, and 7, difficulties are created by: (1) the non-uniform distribution of observations; (2) the similarity of effects on the observations of different gravitational coefficients and station position errors; (3) the inadequacy of the atmospheric model; and (4) the prohibitive

Table 3  
Satellite Orbit Specifications

Orbital Data*	Satellite		
	1960 $\alpha_2$	1959 $\alpha_1$	1959 $\eta$
Epoch	1960 Sept. 22.0	1959 Feb. 28.5	1959 Sept. 28.5
Semi-major axis, $a$ (units of 6378165.m)	1.250057	1.304585	1.334500
Eccentricity, $e$	.011459	.1658200	.1900819
Inclination, $i$	.8243362	.5738098	.5821184
Argument of Perigee, $\omega$	2.263771	3.360617	3.204033
Longitude of Node, $\Omega$	2.281389	2.524415	3.483041
Mean anomaly, $M$	2.728678	6.004626	3.824077
Perigee motion/day, $\dot{\omega}$	+.051863	+.091813	+.085014
Nodal motion/day, $\dot{\Omega}$	-.054127	-.061077	-.057119
Maximum Area-to- Mass ratio ( $\text{cm}^2/\text{gm}$ )	0.27	0.21	0.27
Minimum Area-to- Mass ratio ( $\text{cm}^2/\text{gm}$ )	0.08	0.21	0.04
Perigee height (km)	1500	560	510

\*The six orbital elements at epoch are the constants of integration as defined by Brouwer's theory (Reference 16).

amount of computing time which would be required by a solution taking account of serial correlation between different times. Five methods were suggested to overcome these difficulties:

1. Inclusion of all possible significant perturbations by either physical or empirical models.
2. Preassigned variance and covariance  $V$  for the starting values of parameters for which corrections  $z$  are being determined so that the solution becomes (Reference 4):

$$z = (M^T W^{-1} M + V^{-1})^{-1} M^T W^{-1} f, \quad (12)$$

where  $W$  is the covariance matrix of the observations,  $M$  is the matrix of partial derivatives in the observation equations, and  $f$  is the vector of residuals.

3. Assignment of higher weight to the across-track than to the along-track component of an observation, as described by Equation 3.

4. Observations weighted inversely as their density with respect to phase angles critical for determination of the geodetic parameters, such as node-GST.

5. Use of arbitrary polynomials.

To this list we could add lower weighting—or omission—of observations on days of considerable atmospheric irregularity, according to some index such as the aforementioned  $A_p$ .

The application of the first of these methods is described in the section on dynamics. It was found that inclusion or omission of effects which were secular or of periods more than a few days had very little influence on the values determined for the station shifts or tesseral harmonics. The most troublesome inadequacy was the inability of the empirical atmospheric models to explain orbital variations in the 1.0 to 0.1 cycle per day part of the spectrum. The principal improvement possible would be to utilize the correlation of corpuscularly-caused density variations with the  $A_p$  index (Reference 24).

The second device, specifying variance and covariance for the starting values of the parameters, was necessary to avoid absurdly distorted results due to the ill-conditioning caused by non-uniform distribution of observations coupled with the inadequate accounting for drag effects. For the stations on the Am, EASI, and JKM geodetic systems, the  $9 \times 9$  covariance matrix generated in the solution of Reference 13 was used. For the three isolated datums, the assigned covariance matrices were based on assumed error ellipsoids with  $\pm 35$  m vertical semi-axes in all three cases, and horizontal semi-axes of  $\pm 100$  m for Au;  $\pm 200$  m for Ar; and  $\pm 250$  m for H. The smaller uncertainty for the Australian system is based on the improvement of its position obtained by adjusting deflections-of-the-vertical (Reference 14). For the zonal spherical harmonic coefficients of the gravitational field, the preassigned variances were based on four times the uncertainties given by Kozai (Reference 18). For the tesseral harmonics  $n, m = 2, 1$  and  $2, 2$ , the preassigned variance of  $(2.0 \times 10^{-6})^2$  was based on the order-of-magnitude of earlier determinations of  $J_{22}$  by Kozai (Reference 25), Kaula (Reference 5), and Newton (Reference 26). For the tesseral harmonic coefficients of the third and higher degrees the preassigned  $\sigma$ 's in Table 2 were computed from the degree variances  $\sigma_n^2 \{\Delta g\}$  in Reference 17:

$$\sigma^2 \{ \bar{C}_{nm} \text{ or } \bar{S}_{nm} \} = \frac{\sigma_n^2 \{ \Delta g \}}{(n-1)^2 g^2 (2n+1)} \quad (13)$$

Probably, the principal defect of the preassigned variance technique is a tendency to pre-judge the results—i.e., if two or more parameters have similar effects on the orbit, the solution will tend to be an overestimate for those corrections whose absolute magnitudes are smaller than expected, and an underestimate for those corrections larger than expected. In cases where a series of observations of a satellite were referred to several orbital arcs, the datum and gravitational coefficient variances and covariances were multiplied by the number of orbital arcs, so that the preliminary estimates do not have excessive influence on the final mean value.

The influence of the parameters' preassigned variances and covariances on the result does not depend on their absolute magnitude but rather on their magnitude relative to the variances and covariances specified for the observations. This effect is a consequence of the quadratic sum minimization implied by Equation 12:

$$S = x^T W^{-1} x + z^T V^{-1} z, \quad (14)$$

where  $x$  is the vector of corrections to observations. If the variance assigned to the observations is that based on estimates of purely observational accuracy: direction  $\pm 2''$  (Reference 9); and timing  $\pm 0.002^s$  (Reference 10), then grossly distorted values will be obtained for the geodetic parameters. This distortion is the result of neglecting drag effects. If the covariance, from this drag, between observations a few days apart is not taken into account, the next best solution would be to increase the variance of each observation. The amount of the increase must be found by trial and error. Thus, for example, for satellite 1960.2, initially variances were used of  $(20'')^2 = (10^{-4})^2$  for direction and  $(0.056^s)^2$  for timing over 23-day arcs. Solving a single orbit for all the parameters resulted in rms residuals of  $\pm 4.5'' = \pm 2.2 \times 10^{-5}$  across track and  $\pm 9.7'' = \pm 4.9 \times 10^{-5}$  along track. Since the mean range of the satellite is 2100 km/sec and its motion at right angles to the line of sight (equivalent to the  $C_t$  of Equation 3) averaged about 5.5 km/sec, and since all of the  $\pm 2.2 \times 10^{-5}$  across-track residual is ascribed to directional error, the timing error is

$$\sigma(t) \approx \frac{\bar{r}}{n} \sqrt{\sigma_{\text{along}}^2 - \sigma_{\text{across}}^2} = \frac{2100}{5.5} \sqrt{4.9^2 - 2.2^2} \times 10^{-5} = \pm 0.017^s.$$

A direction variance of  $(2.2 \times 10^{-5})^2$  and a timing variance of  $(0.017^s)^2$  were applied in analyzing all 13 23-day orbital arcs of 1960.2. The resulting corrections to the geodetic parameters are appreciably larger than expected and are listed as "preliminary results" in Tables 1 and 2. Readjusting orbital elements and arbitrary polynomials while holding geodetic parameters fixed obtained rms residuals of  $\pm 13.2'' = \pm 6.45 \times 10^{-5}$  across-track and  $\pm 28.5'' = \pm 1.38 \times 10^{-4}$  along-track. Hence the small residuals for the single 23-arc had been obtained at the expense of distorted geodetic parameters. The observation variances were changed to  $(6.45 \times 10^{-5})^2$  direction and  $(2100 \sqrt{1.38^2 - .645^2} \times 10^{-4} / 5.5)^2 = (0.046^s)^2$  timing for a repeated analysis to obtain the results listed as "final" in Tables 1 and 2.

Table 4 shows the distribution of observations with respect to some angles which appear as arguments of the principal terms in the tesseral harmonics effects. In Table 3 the observations are sorted into 24 sets. The  $n_i$  observations in the  $i$ th set all have the pertinent angle between  $\pi(i-1)/12$  and  $\pi i/12$ . The distribution is far from ideal, but applying weighting factors  $\sum_i n_i / 24 n_j$  appeared to have little effect on the results. For the final analysis of the 1960.2 orbit, weighting with respect to the angle node-GST was applied.

Application of the final device, arbitrary polynomials, was limited to the mean anomaly and to the fourth power in time to avoid the ill-conditioning which occurs in determining the coefficients of higher degree power series. Adding a specification that the orbital residuals should not average more than, say, ten times the  $\pm 20$  m minimum amplitude effect sought sets a limit on the length of the orbital arcs

Table 4

N<sub>i</sub>, Counts of Observation Distribution with Respect to Orbital Angles

Satellite Angle (degrees)	Satellite Observations				
	1960 <sub>α2</sub> (Ω - GST)	1960 <sub>α2</sub> (ω + Ω - GST)	1960 <sub>α2</sub> (-ω + Ω - GST)	1959 <sub>α1</sub> (Ω - GST)	1959 <sub>η</sub> (Ω - GST)
0 - 15	53	40	93	7	2
15 - 30	66	69	48	6	1
30 - 45	67	104	88	6	3
45 - 60	71	97	61	19	17
60 - 75	64	65	65	24	11
75 - 90	89	57	77	19	7
90 - 105	54	56	69	30	12
105 - 120	76	42	74	27	13
120 - 135	41	31	59	46	9
135 - 150	57	47	65	55	14
150 - 165	78	57	89	50	8
165 - 180	66	86	68	27	3
180 - 195	91	56	59	52	19
195 - 210	76	61	47	45	12
210 - 225	92	84	41	31	27
225 - 240	47	66	58	52	23
240 - 255	79	92	53	46	16
255 - 270	79	70	93	58	8
270 - 285	67	55	60	29	11
285 - 300	52	58	64	17	13
300 - 315	50	92	65	30	14
315 - 330	55	92	51	20	4
330 - 345	43	50	69	17	3
345 - 360	49	35	46	14	4
Total	1562	1562	1562	730	254

which can be treated. This limit appeared to be about 23 days for 1960<sub>α2</sub>. The 21-day arcs used for satellites 1960<sub>α1</sub> and 1960<sub>η</sub> resulted in residuals of  $\pm 3.6 \times 10^{-4}$  across-track and  $\pm 4.7 \times 10^{-4}$  along-track, which are appreciably in excess of the limit. However, the 21-day arcs averaged only 35 observations each, and shorter arcs would have had so few observations that an excessive amount of the effects of the geodetic parameters would have been absorbed by the elements of the reference orbit.

To combine the results of several orbital arcs, the more rigorous method would be to use the covariance matrix  $U$  of the corrections to parameters produced by each of the least squares determinations to obtain a generalized weighted mean:

$$\text{Mean } \bar{z} = \left( \sum_i U_i^{-1} \right)^{-1} \sum_i U_i^{-1} z_i . \quad (15)$$

However, the mean solutions obtained in this manner were so distorted that they merely served as a forceful reminder of the falseness of the basic assumption of randomness of observation errors. Hence the solutions given in Tables 1 and 2 were calculated simply by ascribing to each arc a weight proportionate to the total number of observations, in the case of the gravitational coefficients; and proportionate to the number of observations from the datum, in the case of datum shifts. The uncertainties given in the tables are standard deviations computed in the customary manner from the scatter of the results for the different orbital arcs about the mean.

## RESULTS AND CONCLUSIONS

In view of the excessive number of determinations of tesseral harmonics already published, it was resolved not to publish any results which did not satisfy the test that small values were obtained for the harmonics  $\bar{C}_{21}$ ,  $\bar{S}_{21}$ , known to be vanishingly small from latitude variation observations. The analyses of the 1959  $\alpha 1$  and 1959  $\eta$  orbits failed this test. The preliminary results of the 1960  $\alpha 2$  analysis passed the test very satisfactorily, as shown in Table 2, and in the final analysis  $\bar{C}_{21}$ ,  $\bar{S}_{21}$  were held fixed as 0.

Several results show a convincing consistency from orbit-to-orbit: of the 18 datum coordinates, 8 have shifts more than twice their standard deviations while, of the 26 tesseral harmonic coefficients, 7 have magnitudes more than twice their standard deviations. Some of the more marked consistencies, such as the  $\bar{C}_{31}$  coefficient, the southward shift of the Hawaiian station, and the eastward shift of the Argentine station are listed in Tables 5 and 6. The rms magnitudes of the coefficients for the 3rd, 4th, and 6th degrees are 0.50 to 0.70 of what was expected from the autocovariance analysis—indicating perhaps that the variances of the observations should be decreased.

Table 5

Comparison of Results from Different Orbital Arcs of 1960  $\alpha 2$  for Some Datum Shifts in Units of 6.378165 m

Orbit Number	Argentine Datum				Hawaiian Datum			
	Number of Observations	$\Delta u_1$	$\Delta u_2$	$\Delta u_3$	Number of Observations	$\Delta u_1$	$\Delta u_2$	$\Delta u_3$
1	18	+21.0	+12.8	+14.0	2	-30.6	+27.6	-11.6
2	12	+41.6	-20.7	-34.0	14	+22.2	- 3.0	-43.3
3	4	+89.8	-20.2	+10.3	4	+12.6	+17.1	- 7.9
4	6	+46.4	-19.1	-21.5	6	- 9.9	+24.2	-25.8
5	28	+43.7	+23.4	-20.9	3	-10.0	+11.7	-62.0
6	16	+47.9	+ 0.1	-14.1	8	+23.6	+24.9	-47.4
7	7	+39.7	-14.8	- 0.4	19	+10.6	+13.4	-65.5
8	11	+ 7.7	+ 9.3	+18.1	7	+ 0.5	+48.5	-54.0
9	18	+35.4	+24.6	- 5.8	18	-24.4	-16.5	-64.4
10	24	+45.0	-13.6	+23.5	10	-33.6	+78.0	-52.7
11	11	+57.7	-12.6	+13.7	20	+13.2	- 1.6	-58.5
12	13	+17.0	+ 4.2	+18.4	16	+ 6.5	+17.4	-31.9
13	22	+26.0	+ 8.0	+28.9	0			

Table 6  
Comparison of Results from Different Orbital Arcs of 1960,2 for Some Gravitational Coefficients  
(All values multiplied by a scaling factor of  $10^{-6}$ )

Orbit Number	Total Number of Observations	Gravitational Coefficients									
		$\bar{C}_{22}$	$\bar{S}_{22}$	$\bar{C}_{31}$	$\bar{S}_{31}$	$\bar{C}_{41}$	$\bar{S}_{41}$	$\bar{C}_{42}$	$\bar{S}_{42}$	$\bar{C}_{43}$	$\bar{S}_{43}$
1	151	2.50	-0.99	1.86	0.60	-0.50	0.33	1.01	0.55	0.09	0.44
2	161	1.98	-2.64	.61	-.90	.42	1.34	-.35	-.56	.58	-.22
3	73	1.54	-2.90	.75	.28	-.69	.19	-.56	-.26	1.25	.60
4	89	3.54	-1.87	.51	.84	-.33	.86	.98	-.05	-.38	-.14
5	110	1.13	-.68	1.88	-.17	.21	.20	.032	.61	-1.08	-1.76
6	132	2.23	-2.20	1.59	.48	-.90	.07	.14	.22	1.01	.43
7	190	1.82	-1.72	1.66	-.46	.02	.70	.04	.44	1.14	.62
8	109	1.59	-1.07	1.98	-.79	-.53	-.67	-.76	.88	-.07	-.02
9	100	2.33	-1.45	3.73	-1.36	.14	.22	.97	.86	.54	.63
10	118	0.65	-3.94	2.39	.10	-1.31	.72	-.78	-1.06	.029	.21
11	173	1.16	-.80	1.77	.342	-.05	-.04	-.76	1.03	1.46	.83
12	97	2.60	-.27	2.17	.65	.79	1.20	-.065	.97	.82	-.10
13	64	0.90	-2.23	2.72	-1.49	-.38	.67	-.19	.37	.16	-.18

Except perhaps for the equatorial ellipticity,  $n, m = 2, 2$ , good agreement with other recent determinations from either satellite or terrestrial data (References 13, 25, and 27) does not exist. However, for determinations from terrestrial data which are poorly distributed, too much individuality must not be ascribed to the harmonic coefficients; and it is better to make the comparison of spatial, rather than spectral, representations. The geoid in Figure 1 corresponds to the final results given in Table 2. This satellite geoid agrees quite well in the eastern hemisphere with both the gravimetric geoid of Uotila (Reference 27) and the astro-geodetic geoid of Fischer (Reference 28), but in the western hemisphere the agreement is poorer.

Undoubtedly, more information of gravitational variations and station positions can be extracted from existing Baker-Nunn Camera observations. The question is whether it is worth the computational effort, in view of the current or anticipated satellites which will be more frequently observed by Doppler tracking or optical tracking with artificial illumination. Most of the difficulties encountered in the present analysis could be avoided with a satellite of, say, 1000 km perigee height observed an average of 20 or more times a day. However, a more rigorous statistical analysis of a short arc of Baker-Nunn camera observations by the methods described in Reference 6 will be undertaken, as well as the analysis of Doppler observations by the methods described in this paper.

## ACKNOWLEDGMENTS

The author gratefully acknowledges Drs. Fred L. Whipple, George Veis, Yoshihide Kozai, and Mr. Imre G. Izsak, all of the Smithsonian Institution Astrophysical Observatory, for advice and provision of results prior to publication. This work was undertaken at the Smithsonian Institution Astrophysical Observatory, but the bulk of it was accomplished at the Goddard Space Flight Center, with the assistance of Mr. Ed Monasterski and Miss Susan Werner.

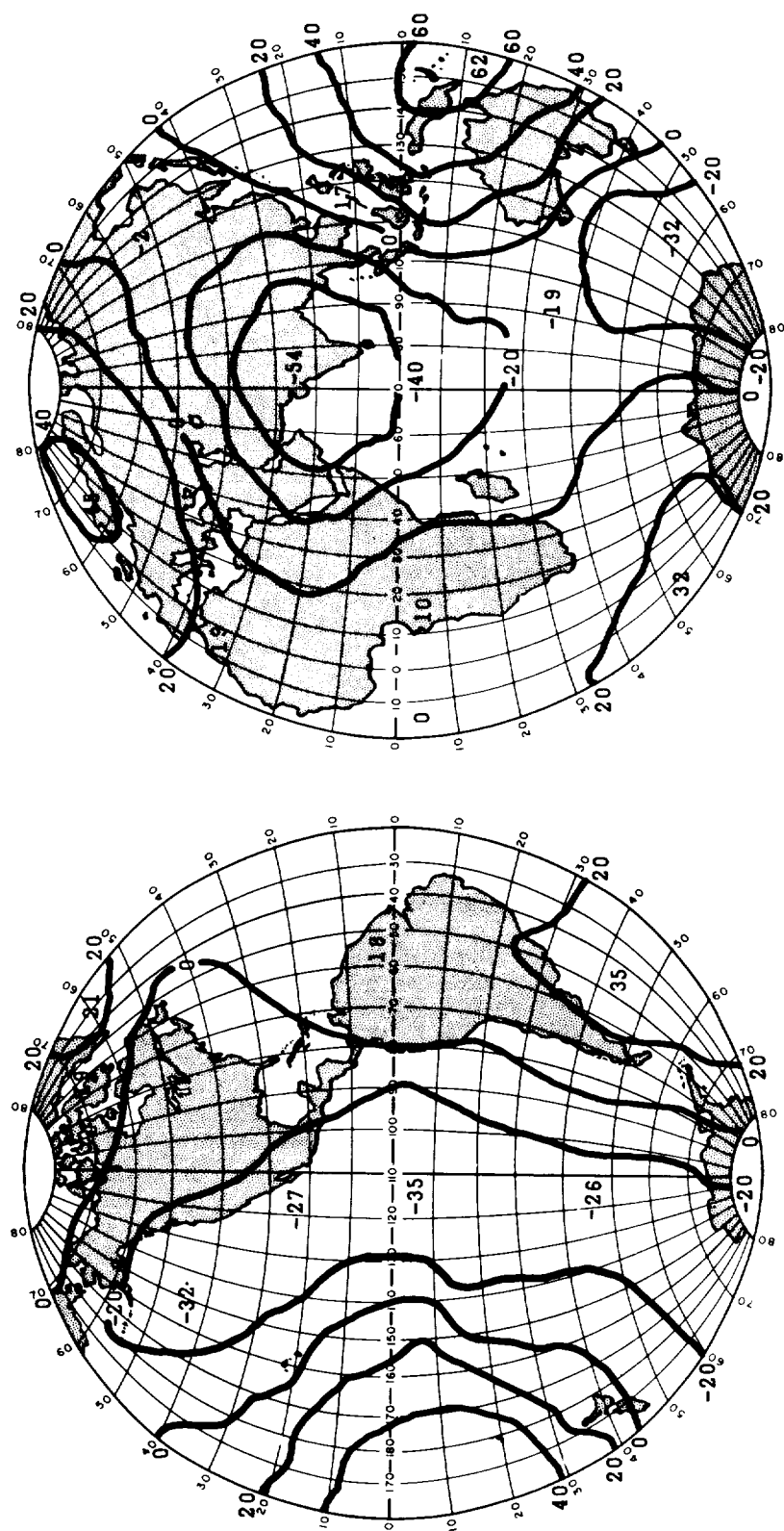


Figure 1—Geoid heights (in meters) referred to an ellipsoid of flattening 1/298.24.

## REFERENCES

1. Veis, G., "Catalog of Precisely Reduced Observations, No. P-1," Smithsonian Inst., Astrophys. Observ., Res. in Space Sci., Spec. Rept. No. 82, November 30, 1961.
2. Veis, G., "Catalog of Precisely Reduced Observations, No. P-2," Smithsonian Inst., Astrophys. Observ., Res. in Space Sci., Spec. Rept. No. 85, February 12, 1962.
3. Haramundanis, K., "Catalog of Precisely Reduced Observations, No. P-4," Smithsonian Inst., Astrophys. Observ., Res. in Space Sci., Spec. Rept. No. 95, June 18, 1962.
4. Kaula, W. M., "Analysis of Gravitational and Geometric Aspects of Geodetic Utilization of Satellites," NASA Technical Note D-572, March, 1961; also *Geophys. J.* 5(2):104-133, July 1961.
5. Kaula, W. M., "Analysis of Satellite Observations for Longitudinal Variations of the Gravitational Field," in: *Space Research II: Proc. 2nd Internat. Space Sci. Sympos., Florence, April 1961*, ed. by H. C. van de Hulst, C. de Jager, and A. F. Moore, Amsterdam: North-Holland Publ. Co., 1961, pp. 360-372.
6. Kaula, W. M., Satellite Orbit Analysis for Geodetic Purposes (in Russian), *Bull. Inst. Theor. Astron: Proc. Conf. on General and Practical Problems of Theoretical Astronomy, Moscow* (in press).
7. Kaula, W. M., "Satellite Orbit Analyses for Geodetic Purposes," in: *Proc. Sympos. on the Dynamics of Satellites, Paris, May 1962*, Berlin: Springer-Verlag (in press).
8. Henize, K. G., "Tracking Artificial Satellites and Space Vehicles," in: *Advances in Space Science*, ed. by F. I. Ordway, III, New York: Academic Press, 1960, Vol. 2, pp. 117-142.
9. Lassovsky, K., "On the Accuracy of Measurements Made upon Films Photographed by Baker-Nunn Satellite Tracking Cameras," Smithsonian Inst., Astrophys. Observ., Res. in Space Sci., Spec. Rept. No. 74, September 18, 1961.
10. Weston, E., "Preliminary Time Reduction for the Determination of Precise Satellite Positions," in: *Catalogue of Precise Satellite Positions*, Smithsonian Inst., Astrophys. Observ., Res. in Space Sci., Spec. Rept. No. 41, May 24, 1960, pp. 11-13.
11. Veis, G. and Whipple, F. L., "Experience in Precision Optical Tracking of Satellites for Geodesy," in: *Space Research II: Proc. 2nd Internat. Space Sci. Sympos., Florence, April 1961*, ed. by H. C. van de Hulst, C. de Jager, and A. F. Moore, Amsterdam: North-Holland Publ. Co., 1961, pp. 17-33.
12. Kaula, W. M., "Celestial Geodesy," in: *Advances in Geophysics*, ed. by H. E. Landsberg and J. Van Mieghem, New York: Academic Press, 1962, Vol. 9, pp. 191-293.
13. Kaula, W. M., "A Geoid and World Geodetic System Based on a Combination of Gravimetric, Astrogeodetic, and Satellite Data," *J. Geophys. Res.* 66(6):1799-1811, June 1961.

14. Veis, G., "The Positions of the Baker-Nunn Camera Stations," Smithsonian Inst., Astrophys. Observ., Res. in Space Sci., Spec. Rept. No. 59, March 3, 1961.
15. Brouwer, D., "Solution of the Problem of Artificial Satellite Theory Without Drag," *Astronom. J.* 64(1274):378-397, November 1959.
16. Brouwer, D. and Clemence, G. M., "Methods of Celestial Mechanics," New York: Academic Press, 1961.
17. Kaula, W. M., "Statistical and Harmonic Analysis of Gravity," *J. Geophys. Res.* 64(12):2401-2421, December 1959.
18. Kozai, Y., "The Potential of the Earth Derived from Satellite Motions," in: *Proc. Sympos. on the Dynamics of Satellites, Paris, May 1962*, Berlin: Springer-Verlag (in press).
19. Kaula, W. M., "Development of the Lunar and Solar Disturbing Functions for a Close Satellite," NASA Technical Note D-1126, January 1962; also *Astronom. J.* 67(5):300-303, June 1962.
20. Jacchia, L. G., "A Variable Atmospheric-Density Model from Satellite Accelerations," *J. Geophys. Res.* 65(9):2775-2782, September 1960.
21. Harris, I. and Priester, W., "Time-Dependent Structure of the Upper Atmosphere," NASA Technical Note D-1444, August 1962.
22. O'Keefe, J. A., Eckels, A., and Squires, R. K., "The Gravitational Field of the Earth," *Astronom. J.* 64(7):245-253, September 1959.
23. Kozai, Y., "Second-Order Solution of Artificial Satellite Theory without Air Drag," *Astronom. J.* 67(7):446-461, September 1962.
24. Jacchia, L. G., "Electromagnetic and Corpuscular Heating of the Upper Atmosphere," in: *Space Research III: Proc. 3rd Internat. Space Sci. Sympos., Washington, May 1962*, Amsterdam: North-Holland Publ. Co. (To be published).
25. Kozai, Y., "Tesseral Harmonics of the Gravitational Potential of the Earth as Derived from Satellite Motions," *Astronom. J.* 66(7):355-358, September 1961.
26. Newton, R. R., "Ellipticity of the Equator Deduced from the Motion of Transit 4A," *J. Geophys. Res.* 67(1):415-416, January 1962.
27. Uotila, U. A., "Corrections to Gravity Formula from Direct Observations and Anomalies Expressed in Lower Degree Spherical Harmonics," Ohio State Univ., Inst. of Geodesy, Photogrammetry and Cartography Rept. No. 23, 1962.
28. Fischer, I., "An Astrogeodetic World Datum from Geoidal Heights Based on the Flattening  $f = 1/298.3$ ," *J. Geophys. Res.* 65(7):2067-2076, July 1960.

